JOURNAL OF Materials CHEMISTRY

Synthesis and characterization of graphite-like B–C–N materials of composition $CN_x(BN)_y$ ($x \ll 1$, $y \leqq 1$)

Tamikuni Komatsu*[a] and Akiko Goto[b]

[a]*c/o National Institute of Advanced Industrial Science and Technology FCT Laboratory Research Center, Asahi Kasei Corporation, 1-1 Higashi, Tsukuba-shi, Ibaraki, 305, Japan. E-mail: BRA01367@nifty.ne.jp*

[b]*National Institute of Advanced Industrial Science and Technology FCT Laboratory Research Center, 1-1 Higashi, Tsukuba-shi, Ibaraki, 305, Japan*

Received 15th August 2001, Accepted 28th January 2002
First published as an Advance Article on the web 19th March 2002

Various graphite-like B–C–N materials were synthesized in the precursor pyrolysis system of boron trichloride and nitrogen-containing materials such as heptaazaphenalene derivatives, carbodiimides, amines, nitriles and cyanamides. The materials obtained were described with a formula of $CN_x(BN)_y$ and $CB_x(BN)_y$ consisting of CN_x and $(BN)_y$ segments. A combination of chemical decomposition and structural analysis elucidated that the segment structure of $CN_x(BN)_y$ contains local bonds of $(–C{=}C–)_n–N\lessgtr$, B–N–C and B–N pairs but no C–B bonds. A miscible blend structure model was expected by analogy with hybrid materials. Compositions and yields of the materials were closely related to the properties of chemical reaction, nitrogen evolution and graphitization of the starting materials. In particular, B–C–N materials with high BN content were prepared in small quantities from the heptaazaphenalene polymers, and the materials with low BN content were produced from teteracyanoethylene in nearly 100% yield. The materials were oxidized to boron oxide from 500 °C to 950 °C, however, under an inert atmosphere they were stable to at least 1200 °C.

Graphite-like B–C–N materials, g-B–C–N, are useful as the precursors of cubic B–C–N hard materials[1–3] and semiconductive B–C–N nanotubes.[4,5] A variety of g-BC_xN ($x \geq 1$) materials have been prepared by solid–gas reaction,[6,7] precursor pyrolysis[8–10] and mainly by chemical vapor deposition (CVD).[11–15] Derre *et al.* described the CVD-synthesized g-B–C–N materials with a ternary diagram as two formulae: the $C(BN)_xB_y$ (x, $y \leqq 1$) composed of sp^2 carbon, B–N pairs and excess amounts of boron; the $C(BN)_x$ ($x \leqq 1$) composed of sp^2 carbon and B–N pairs.[14] Since a triangular C–BN–N part of this diagram (an area connected by the three points C, BN and N) has been almost empty, it is of interest to develop new B–C–N materials with rich B–N content hidden in the C–BN–N part. However, a number of C–N materials usually undergo predominant evolution of elemental nitrogen during carbonization, so the production of B–N rich materials is very difficult. The solid–gas reaction and precursor pyrolysis methods are based on the chemical reactions that first form the Lewis acid–base adducts between boron starting materials such as boron halides and hydrides and carbon–nitrogen starting materials such as amines and nitriles, followed by pyrolytic carbonization with evolution of hydrogen halides or hydrogen. For the purpose of industrial uses of the above B–C–N hard materials and semiconductive materials, bulk synthesis of their precursors, g-B–C–N materials, is essential. However, useful methods are almost unknown except for the preparation of g-BC_3N[7] by solid–gas reaction between polyacrylonitrile and BCl_3. Since g-B–C–N materials are compositionally related to boron carbide, boron nitride and carbon nitride, it may be possible to make chemical changes among them. Numerous carbon nitride CN_x powders, films, nanotubes[16] and nanofibers[17] have been reported, but most of them were amorphous and contained small amounts of nitrogen. Recently, we prepared a series of C_3N_4-like polymers composed of heptaazaphenalene.[18–20] The polymers were found to react with boron halides and change into new g-B–C–N materials of high BN content. This reaction system was further extended to various N-containing materials for the purpose of bulk synthesis of the B–C–N materials. In this work, these results were reported.

Experimental

Sample preparation

1,3,4,6,7,9,9b-Heptaazaphenalene-2,5,8-triamine [melem: $C_6N_7(NH_2)_3$][18] and its derivatives such as the decamer of melem [$-(C_6N_7)(NH_2)(NH)-]_{10}$,[18] highly-deammonated polycondensates of melem (prototype C_3N_4: [$-C_6N_7(NH)-(N)C_6N_7(N)-$]),[18] 1,3,4,6,7,9,9b-heptaazaphenalene-2,5,8-tricarbodiimide [hydromelon acid: $C_6N_7(NCNH)_3$][19] and its copper salt [copper melonate: $C_6N_7(NCN)_3{\cdot}1.5\ Cu$],[19] amines such as melamine, melamine–formaldehyde resin, urea–formaldehyde resin and hexamethylenetetramine (hexamine), nitriles such as tetracyanoethylene (TCNE), polyacrylonitrile (PAN), diaminomaleonitrile, malononitrile, adiponitrile and dicyanodiamide, cyanamides such as zinc cyanamide, were used as C–N starting materials. Melem and its derivatives were prepared according to the synthetic routes reported previously.[18,19] The other compounds were commercially available. The B–C–N samples were prepared using an apparatus consisting of a three-necked separable quartz flask equipped with a gas-admitting tube, mechanical quartz stirrer and vent tube and a furnace (Fig. 1). Many of the samples were prepared from the BCl_3 adducts of the C–N starting materials. The adducts were prepared by introducing BCl_3 gas into a solution of the starting materials. From melamine, hexamine, PAN, adiponitrile and dicyanodiamide, white adducts sensitive to moisture were obtained. TCNE, diaminomaleonitrile and malononitrile underwent rapid polymerization under an atmosphere of BCl_3 gas in the usual solvents such as toluene and turned to soluble black-purple polymer–BCl_3 adducts. These adducts were heated in a stream of BCl_3 gas up to a maximum temperature of 1000 °C at a heating rate of *ca.*

 DOI: 10.1039/b107419a

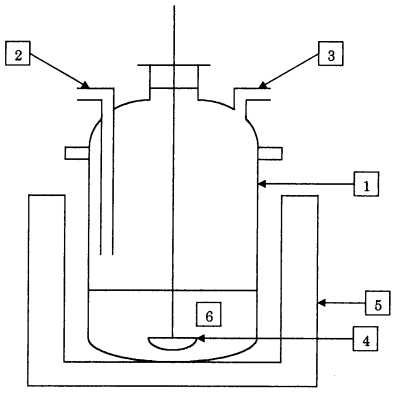

Fig. 1 The apparatus used for the preparation of the B–C–N materials: 1, three-necked separable quartz flask; 2, quartz tube for admitting BCl_3 and N_2 gas; 3, quartz vent leading to a draught chamber; 4, mechanical quartz-stirrer; 5, electric furnace controlled by a thermocouple; 6, sample.

20 °C min^{-1}, held for 30 min, and purged with N_2 gas at 1000 °C until all volatile products were expelled. Melem and its derivatives, amino resins and zinc cyanamide were directly heated in a stream of BCl_3 gas, held for 30 min and purged with N_2 gas. These crude products were purified by boiling in 5% NaOH and 10% HCl, washed with boiling water and vacuum-dried at 500 °C. The crude product from copper melonate was boiled in 20% HNO_3 to remove copper salts before the above treatment. Several B–C–N materials obtained were hydrolyzed by boiling in 30% HNO_3, boiling in 10% NaOH, neutralized with dil. HCl, followed by CHN analysis, IR and XPS measurements. For comparison, carbonaceous materials containing small amounts of nitrogen (carbonaceous CN_x) were prepared by pyrolysis of a TCNE polymer and PAN in a stream of N_2 gas at 1000 °C. The TCNE polymer was prepared by reflux/dry heating (400 °C) of a toluene–THF solution of TCNE and $ZnCl_2$, according to the reported method.[21] Quasi boron nitride, $CH(BN)_{5.13}$, was prepared by pyrolysis of a diethylamine–BCl_3 adduct and g-BC_4N was synthesized according to the CVD method.[7,15]

Measurements

The CHN contents of the samples were measured using a Perkin-Elmer 2400 II CHNS/O elemental analyzer. For the B content, the sample (0.1 g) was mixed with K_2CO_3 (1.0 g) and Na_2CO_3 (1.0 g), placed in a Pt crucible, completely melted using a burner, cooled to room temperature, dissolved in 35% HCl, diluted with ultrapure water, and the $B(OH)_3$ present was determined using a VG-Elemental Plasmatrace ICP-mass analyzer. IR spectra were measured in KBr disk form using a Simazu FT-IR 8200 PC spectrometer. Raman spectra were measured at an excitation wavelength of 1064 nm generated with a 150 mW Nd–YAG laser using a Perkin-Elmer FT-Raman 2000 spectrometer. X-Ray photoelectron spectroscopy was carried out using monochromated Al-Kα X-ray radiation (1486.5 eV) and the photoelectrons were detected by a hemispherical analyzer operating at a pass energy of 23.5 eV using an Ulvac-Phi ESCA 1700S spectrometer. The binding energy was calibrated on the reference Au ($4f_{7/2}$) peak at 83.98 eV, and XPS curve fitting was performed with a non-linear least-squares fitting program using a mixed Gaussian–Lorentzian product function. X-Ray powder diffraction was conducted in the 2θ range 4–100° with Cu-Kα radiation generated at 40 kV–200 mA at a scanning speed of 0.25° min^{-1} using a Rigaku RINT-2500 X-ray powder diffractometer. The powder pattern obtained was smoothed using a smoothing program, LOW PASS FILTER, installed in a machine to determine the precise peak positions. DSC-TG measurements were carried out up to 1200 °C at a heating rate of 20 °C min^{-1} in a stream of argon and air with a flow volume of 100 ml min^{-1} using a TA-Instrument SDT 2960 DSC-TGA. Density was measured by the sink–float method in a dibromomethane–ethanol solution whose density was determined pycnometrically. As standard materials, graphite, vitreous carbon and hexagonal boron nitride (h-BN)were used.

Results and discussion

All the B–C–N samples contained large amounts of carbon, nitrogen and boron and small amounts of hydrogen (Table 1). IR spectroscopy measured very small NH stretching bands around 3160 cm^{-1}, even for the B–C–N samples prepared from the hydrogen free starting materials such as TCNE, copper melonate and zinc cyanamide. For several samples, XPS analysis detected a very small C_{1s} peak at 289–92 eV due to carbonyl groups of adsorbed contaminants and surface oxidation products, since the peaks were decreased by Ar^+ ion-beam sputtering, but none of the peaks due to the oxygen-containing C=O, B=O, B–OH, N=O and N–O groups were observed by IR spectroscopy. The hydrogen and oxygen components arise from surface impurities of the B–C–N samples, therefore, both components are not essential for the structural characterization of the B–C–N materials. Chemical

Table 1 Compositions and yields of the B–C–N materials prepared from various starting materials

Starting materials	Method[a] A or D	BCl_3 Temp/°C	N_2 Temp/°C	C/H/N/B content (%) C	H	N	B	B–C–N Composition	Yield/%
$C_6N_7(NH_2)_3$ Melem	D	1000	1000	24.76	0.91	41.77	32.56	$CB_{1.46}N_{1.45}$	7
$[-(C_6N_7)(NH_2)(NH)-]_{10}$ Decamer of melem	D	1000	1000	32.80	0.98	39.83	26.39	$CB_{0.89}N_{1.04}$	5
$[-C_6N_7(NH)(N)-C_6N_7(N)-]_n$ Prototype carbon nitride	D	1000	1000	21.64	1.39	43.35	33.62	$CB_{1.73}N_{1.72}$	2
$C_6N_7(NCNH)_3$ Hydromelon acid	D	600	1000	33.89	0.29	35.21	30.61	$CB_{1.00}N_{0.89}$	10
$C_6N_7(NCN)_3{\cdot}1.5Cu$ Copper melonate	D	800	1000	64.05	0.39	20.62	14.93	$CB_{0.26}N_{0.28}$	5
Melamine	A	1000	1000	31.98	2.21	37.85	27.96	$CB_{0.97}N_{1.01}$	10
Melamine resin	D	1000	1000	45.44	2.61	31.91	20.04	$CB_{0.49}N_{0.60}$	19
Urea resin	D	1000	1000	62.55	1.45	20.58	15.42	$CB_{0.27}N_{0.28}$	15
Hexamine	A	1000	1000	65.96	0.35	20.62	13.06	$CB_{0.22}N_{0.27}$	35
TCNE	A	1000	1000	69.61	0.63	17.87	11.90	$CB_{0.19}N_{0.22}$	98
PAN	A	1000	1000	67.86	0.61	18.75	12.77	$CB_{0.21}N_{0.22}$	75
Diaminomaleonitrile	A	650	1000	62.09	2.43	21.23	14.25	$CB_{0.28}N_{0.29}$	70
Malononitrile	A	650	1000	62.07	1.60	17.89	18.44	$CB_{0.33}N_{0.25}$	60
Adiponitrile	A	1000	1000	72.28	0.60	15.01	12.10	$CB_{0.19}N_{0.18}$	50
Dicyanodiamide	A	1000	1000	73.53	0.28	15.01	11.18	$CB_{0.17}N_{0.18}$	10
Zinc cyanamide	D	800	1000	24.02	0.14	48.21	27.63	$CB_{1.28}N_{1.72}$	6

[a]The symbols A and D denote a BCl_3 adduct of the starting material and an unmodified form used as starting material, respectively.

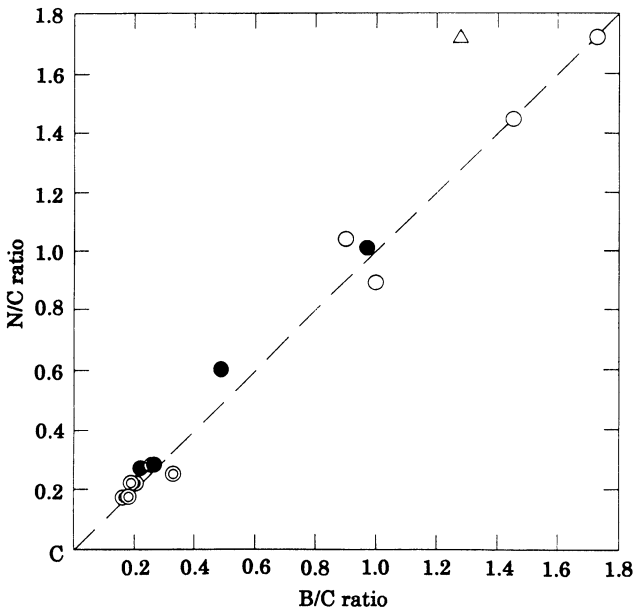

Fig. 2 Plots of the compositions of the B–C–N materials prepared from various C–N resources: (○), heptaazaphenalene derivatives; (●), amines; (◎), nitriles; (△), cyanamide.

compositions and yields of the B–C–N materials greatly depended on the starting materials (Table 1). The aromatic N-rich amines such as heptaazaphenalene derivatives that are resistive to nitrogen evolution during carbonization produced small amounts of new B–C–N materials exhibiting very high B/N content as never known. On the other hand, the aliphatic N-rich amines and nitriles gave low B/N content. The yields of the B–C–N materials were specifically related to the starting materials. Nitriles such as TCNE and PAN that are easily graphitized gave them in very high yields. The use of the BCl_3 adducts usually produced them in more satisfactory yield than the direct method. The B–C–N materials obtained were classified using a coordination diagram described with point C_1 at the origin, N/C ratio on the *y*-axis and B/N ratio on the *x*-axis (Fig. 2). The diagonal line passing the origin shows a composition of $C(BN)_x$. It is noted that most of the B–C–N materials are distributed in the region slightly above the diagonal line. Small numbers of the materials from the heptaazaphenalene derivatives and malononitrile are in the region below the line. Namely, the materials are described with a formula of $CN_x(BN)_y$ and $CB_x(BN)_y$ consisting of a large portion of BN pairs and slight excesses of N or B elements.

IR spectra of all the B–C–N materials were similar in appearance to the spectrum of a mixture of carbonaceous CN_x and boron nitride, as seen in the hybridization of C=N and C=C bonds at 1600–1558 cm^{-1} and sp^2 B–N bonds at 1400 cm^{-1} (Fig. 3). The B–N bonds are, however, somewhat different from a pure B–N bond of h-BN, because the 1400 cm^{-1} peak is shifted 27 cm^{-1} to higher wavenumber from the peak of h-BN. This shift is much larger than those arising from fine carbon particles present in h-BN (the shift even for the quasi boron nitride containing 8% carbon was at most 10 cm^{-1}). The large shift indicates chemical bonds between the CN_x and BN segments. The Raman spectra showed very broad peaks around 1590 and 1360 cm^{-1} that are usually assigned to G and D bands, respectively. No relation between band shifts and BN contents was observed. Since the relative G/D intensities were less than 1.0, an ill-ordered structure and the influence of very different vibrational modes when compared to pure graphite were suggested. The XPS B_{1s},C_{1s} and N_{1s} signals appeared at 190.8–191.8 eV, 284.5–285.7 eV and

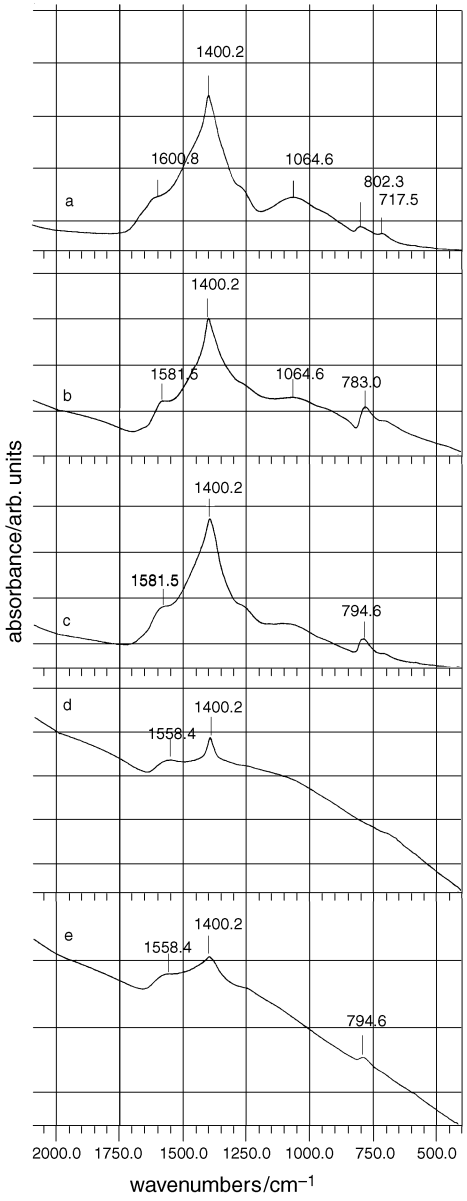

Fig. 3 IR spectra of the representative B–C–N materials: (a), $CB_{1.73}N_{1.72}$ prepared from prototype C_3N_4; (b), $CB_{1.00}N_{0.89}$ from hydromelon acid; (c), $CB_{0.97}N_{1.01}$ from melamine; (d), $CB_{0.19}N_{0.22}$ from TCNE; (e), $CB_{0.21}N_{0.22}$ from PAN.

398.3–398.8 eV; these were shifted to slightly higher energies than the values of 190.4 eV for h-BN, 284.5 eV for vitreous carbon and 398.0 eV for h-BN, respectively (Fig. 4). Each signal was curve-fitted with several peaks, which suggests diversity in bonding modes of each element (Table 2). It has been reported that the CVD-synthesized g-BCN and g-BC_3N materials have local structures of $B(C)_3$, $B(N–C)_3$ and B–N–C on the basis of the B_{1s} peaks at 189.4–5 eV and 192.1 eV and the N_{1s} peak at 399.1–3 eV, respectively.[15] Also, the $\rangle$C=C–N$\langle$ and $\rangle$C=N– bonds of the g-CN_x derived from heptaazaphenalene showed C_{1s} peaks at 286.0 and 287.7 eV and N_{1s} peaks at 400.5 and 398.5 eV respectively.[20] Since the B–C–N materials in this work show the deconvolution peaks at 191–192, 285–286 and 399–400 eV, there may be local structures of $B(N–C)_3$, B–N–C and $(–C=C–)_n–N\langle$ (the C_{1s} binding energy being slightly lower than that of g-CN_x shows an increase in resonance effect with an increase in number of sp^2 carbons, which suggests $(–C=C–)_n–N\langle$ bonds rather than the $\rangle$C=C–N$\langle$ bond), but no structures of $B(C)_3$ and $\rangle$C=N– (Table 2). The density was 1.7–1.9 g cm^{-3}, much smaller than that of vitreous carbon. All the B–C–N materials showed broad X-ray powder diffraction

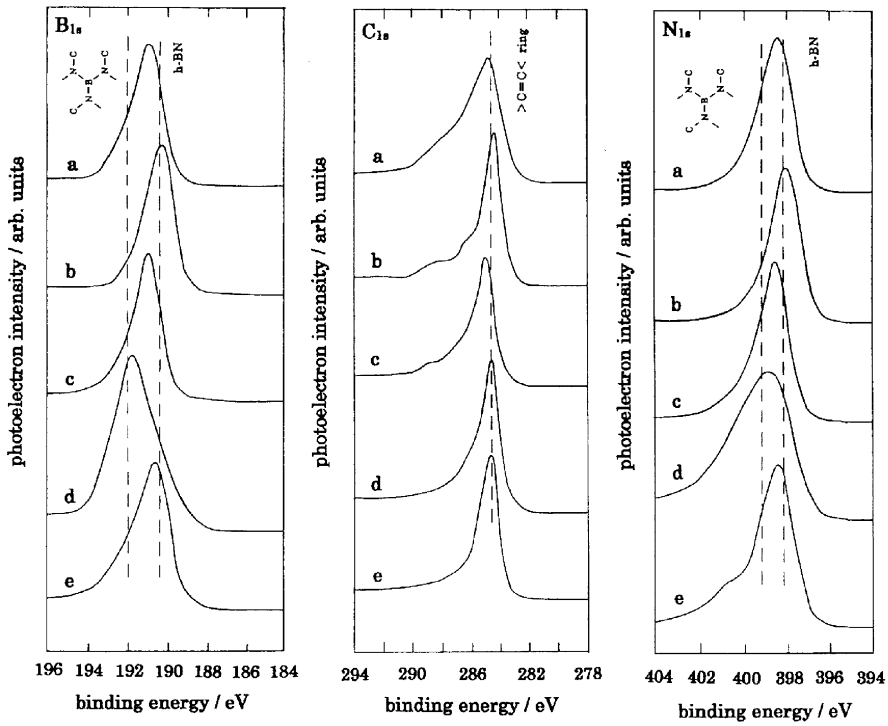

Fig. 4 XPS B_{1s}, C_{1s} and N_{1s} spectra of the representative B–C–N materials: (a), $CB_{1.73}N_{1.72}$ prepared from prototype C_3N_4; (b), $CB_{1.00}N_{0.89}$ from hydromelon acid; (c), $CB_{0.97}N_{1.01}$ from melamine; (d), $CB_{0.19}N_{0.22}$ from TCNE; (e), $CB_{0.21}N_{0.22}$ from PAN.

Table 2 XPS B_{1s}, C_{1s} and N_{1s} binding energies of the representative B–C–N materials and the standard materials[a]

B–C–N materials (starting materials)	B_{1s} Main peak/eV Fitting (% area)	C_{1s} Main peak/eV Fitting (% area)	N_{1s} Main peak/eV Fitting (% area)
$CB_{1.73}N_{1.72}$ (Prototype carbon nitride)	**190.9** 190.8 (81) 192.1 (19)	**284.7** 284.6 (14) 286.3 (66) 288.0 (20)	**398.3** 398.2 (41) 398.9 (59)
$CB_{1.00}N_{0.89}$ (Hydromelon acid)	**190.2** 190.2 (71) 191.4 (20)	**284.3** 284.3 (63) 285.8 (22) 288.0 (15)	**397.9** 397.9 (80) 399.1 (20)
$CB_{0.97}N_{1.01}$ (Melamine)	**191.0** 190.9 (48) 191.5 (52)	**284.9** 284.9 (27) 285.4 (56) 288.0 (17)	**398.5** 398.3 (57) 399.4 (43)
$CB_{0.19}N_{0.22}$ (TCNE)	**191.8** 190.6 (38) 191.9 (62)	**284.5** 284.4 (32) 285.1 (42) 287.1 (21)	**398.8** 398.4 (39) 399.8 (43) 401.6 (12)
$CB_{0.21}N_{0.22}$ (PAN)	**190.6** 190.6 (73) 192.0 (27)	**284.6** 284.6 (50) 285.5 (40)	**398.3** 398.3 (57) 399.8 (43)
g-BC_4N	**190.1** 188.8 (13) 190.1 (80)	**284.6** 283.1 (11) 284.1 (21) 284.9 (44) 286.1 (17)	**397.7** 397.7 (51) 398.2 (49)
h-BN	**190.4** 190.3 (49) 190.6 (51)		**398.0** 397.9 (52) 398.2 (48)
Vitreous carbon		**284.5** 284.5 (71) 285.0 (19)	

[a]Observed and curve-fitted peaks. Numbers in bold indicate observed peak positions.

patterns characteristic of turbostratic carbon-based materials such as g-BCN,[7] g-BC_3N,[15] g-CN_x[20] and vitreous carbon (Fig. 5). The patterns could be assigned in appearance to a hexagonal crystal system as well as the above materials. The

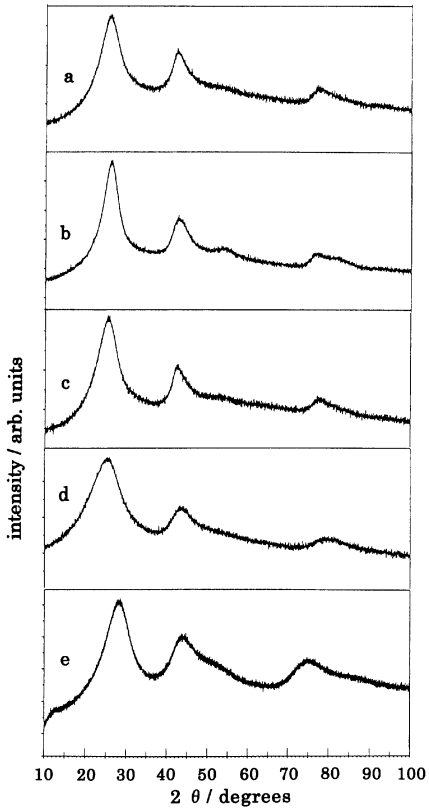

Fig. 5 X-Ray powder diffraction of the representative B–C–N materials: (a), $CB_{1.73}N_{1.72}$ prepared from prototype C_3N_4; (b), $CB_{1.00}N_{0.89}$ from hydromelon acid; (c), $CB_{0.97}N_{1.01}$ from melamine; (d), $CB_{0.19}N_{0.22}$ from TCNE; (e), $CB_{0.21}N_{0.22}$ from PAN.

lattice constants a_0 and c_0 were estimated to be between those of vitreous carbon and quasi boron nitride depending on the BN content (Table 3). The unit cell volume calculated was 0.035–0.036 nm^3 or 96–100% of the volume of vitreous carbon. The total atomic mass in the unit cell was 36–41 g or 75–85% of the mass of vitreous carbon. These results were also confirmed for the CVD synthesized g-BC_4N material. The low density is responsible for this considerable mass deficiency. There must be many structural defects.

Boiling in 30% HNO_3 did not decompose carbonaceous CN_x and graphite-like carbon nitrides, on the other hand, the B–C–N samples decomposed into a residue of carbonaceous CN_x and alkali-soluble quasi boron nitrides and boric acid. Prolonged hydrolysis increased the quantities of boric acid and finally gave a residue of CN_x ($x \ll 1$). This means that HNO_3 hydrolysis of the B–C–N samples enables selective bond cleavage between CN_x segments and $(BN)_y$ segments. The dissociated BN segments are further hydrolyzed into boric acid. For example, hydrolysis of the $CB_{0.91}N_{1.04}$ materials from melamine gave a $CB_{0.12}N_{0.22}$ residue having lost a $(BN)_{0.80}$ segment and considerable amounts of boric acid and ammonium nitrate. Accordingly, the large BN loss after hydrolysis shows that the B–C–N material has a segment structure of CN_x–$(BN)_y$. The hydrolyzed residue for the $CB_{0.19}N_{0.22}$ material from TCNE showed a composition of $CN_{0.053}$ similar to the pyrolytic $CN_{0.053}$ derived from the TCNE polymer. Both materials were characterized by XPS; the C_{1s} and N_{1s} spectra of the two materials were the same. This was also confirmed for the B–C–N material from PAN. Namely, the structure of the CN_x segments of the B–C–N materials is controlled by carbonization of the starting materials.

The B–C–N materials were classified into at least two types from the DSC-TG measurements in a stream of air (Fig. 6). The materials from the heptaazaphenalene derivatives and melamine decreased in weight in the range 500 to 750 °C, reached a plateau from 750 °C to 850 °C, but in the range 850–950 °C appreciably increased in weight. Two large exothermic peaks corresponding to the above weight loss and gain were observed. IR and elemental analysis of the TG residue at each stage elucidated that the first decrease is due to oxidative decomposition of the CN_x segment and the next increase is due to oxidation of the $(BN)_y$ segment into $(BO)_y$. Since the quasi boron nitride also shows analogous TG behavior, such a thermal property may be characteristic of the B–C–N materials with rich BN contents. On the other hand, the materials from the nitriles and aliphatic amines decreased in weight in the range 500 to 800 °C, and slightly increased or decreased in weight above 800 °C. A large exothermic peak corresponding to the large weight loss appeared at 600 °C, however, an exothermic peak appearing over 800 °C was very weak. The TG residue at 850 °C was a mixture of boron oxide and small amounts of carbonaceous materials. The results mean that the CN_x and $(BN)_y$ segments are oxidized at the same time. The B–C–N materials showing such a TG behavior are not a mixture of graphite and h-BN that loses a graphite component in the range 700 to 950 °C and leaves a residue of only h-BN above 950 °C. In an inert atmosphere, the B–C–N materials showed high heat resistance up to at least 1200 °C, owing to the graphite-like fused structure.

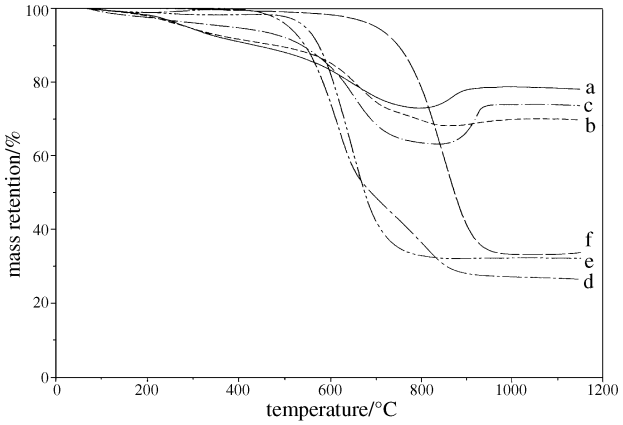

Fig. 6 Thermogravity of the representative B–C–N materials: (a), $CB_{1.73}N_{1.72}$ prepared from prototype C_3N_4; (b), $CB_{1.00}N_{0.89}$ from hydromelon acid; (c), $CB_{0.97}N_{1.01}$ from melamine; (d), $CB_{0.19}N_{0.22}$ from TCNE; (e), $CB_{0.21}N_{0.22}$ from PAN; (f), a 2 : 1 w/w mixture of graphite and h-BN. The experiments were conducted in the range 30–1200 °C in a stream of air.

Several structural models of g-BCN, g-BC_2N and g-BC_3N, in which their chemical structures consist of the same repeating units as the chemical compositions, have been presented on the assumption that they are pure and single phase materials.[15,22–24] The B–C–N materials in this work are far from a single phase like the above g-BC_xN ($x = 1, 2, 3$) but not a mixture. Under the limited conditions that a large portion of the B and N elements are used as BN pairs and there are B–N–C, $(–C{=}C–)_n–N\lessgtr$, and B–N bonds but no C–B bonds, how are the CN_x and $(BN)_y$ segments connected without additional

Table 3 Compositions, density, lattice constants, unit cell volume and mass/unit cell volume of the B–C–N materials prepared from various starting materials

Starting materials	B–C–N material composition	ρ/g cm^{-3}	Lattice constants		Volume/nm^3	Mass/g mol^{-1}
			a_0/nm	c_0/nm		
Melem	$CB_{1.46}N_{1.45}$	1.72	0.244	0.697	0.036	37
Decamer of melem	$CB_{0.89}N_{1.04}$	1.96	0.244	0.695	0.036	42
Prototype C_3N_4	$CB_{1.73}N_{1.72}$	1.79	0.245	0.696	0.036	39
Hydromelon acid	$CB_{1.00}N_{0.89}$	1.83	0.244	0.682	0.035	39
Copper melonate	$CB_{0.26}N_{0.28}$	1.82	0.243	0.676	0.035	38
Melamine	$CB_{0.97}N_{1.01}$	1.88	0.245	0.696	0.036	41
Melamine resin	$CB_{0.49}N_{0.60}$	1.74	0.244	0.681	0.035	37
Urea resin	$CB_{0.27}N_{0.28}$	1.76	0.242	0.698	0.035	38
Hexamine	$CB_{0.22}N_{0.27}$	1.70	0.240	0.708	0.035	36
TCNE	$CB_{0.19}N_{0.22}$	1.81	0.240	0.698	0.035	38
P AN	$CB_{0.21}N_{0.22}$	1.71	0.238	0.696	0.034	35
Dicyanodiamide	$CB_{0.17}N_{0.18}$	1.71	0.242	0.693	0.035	36
Standard materials						
g-BC_4N	$CB_{0.28}N_{0.25}$	1.75	0.243	0.700	0.036	38
Vitreous carbon	C	2.19	0.239	0.737	0.036	48
Quasi boron nitride	$CHB_{5.13}N_{5.13}$	1.94	0.247	0.672	0.036	42

nitrogen? From the result of HNO_3 hydrolysis, it is almost certain that the both segments are aggregated. Since only the terminal boron of the BN segment is bonded to the nitrogen of the CN_x segment, the two segments can be linked by the least amounts of nitrogen. The aggregation of the two segments is believed to be associated with the mechanism that the C–N and B–N bonds of the starting precursors cyclize, fuse and coagulate individually during the course of carbonization. By analogy with hybrid materials such as polymer alloys, a miscible blend structure consisting of two compatible segments, in which the BN segment is homogeneously micro-dispersed in the carbon matrix, is presented. Another possibility is the separated C/BN layered structure that was assigned to the arc-discharged B–C–N nanotubes.[25–27] However, this structure may be inappropriate to the present B–C–N materials, because the two segments are not completely separated. The $(BN)_y$ segments of the B–C–N materials must be small in size, considering their oxidative instability. The structure of $CB_x(BN)_y$ is not clear at present. The materials from hydromelon acid and malononitrile were hydrolyzed, however, each carbonaceous residue contained no boron. The amounts of C–B bonds may be so small that the bonds cannot be detected, although it seems possible that BCl_3 undergoes electrophilic addition to carbon atoms of the carbodiimide and nitrile groups.

Conclusion

Various graphite-like B–C–N materials were synthesized by precursor pyrolysis of boron trichloride and nitrogen-containing starting materials such as heptaazaphenalene derivatives, carbodiimides, amines, nitriles and cyanamides. The B–C–N materials obtained were described with a formula of $CN_x(BN)_y$ and $CB_x(BN)_y$. XPS and IR spectroscopy and HNO_3 hydrolysis of the materials elucidated that the materials are composed of CN_x and $(BN)_y$ segments and combined with local bonds of $B(N–C)_3$, B–N–C, $(–C=C–)_n–N<$ and BN pairs but no C–B bonds. By analogy with hybrid materials, a miscible blend structure in which the BN segment is homogeneously micro-dispersed in the CN_x matrix was proposed. All the materials have a turbostratic hexagonal structure containing many defects. Chemical compositions and yields of the B–C–N materials were related to the properties of chemical reactions, nitrogen-evolution and graphitization of the starting materials. For example, the heptaazaphenalene derivatives that are resistive to nitrogen evolution during carbonization gave the $CB_x(BN)_y$ type with rich B/N contents, nitriles such as tetracyanoethylene that is readily graphitizable produced the $CN_x(BN)_y$ and $CB_x(BN)_y$ types in high yields, and amines yielded the $CN_x(BN)_y$ type in moderate yields. The materials were oxidized above 500 °C in a stream of air and finally changed into boron oxide; however, in an inert atmosphere they were stable to at least 1200 °C.

Acknowledgement

This work was conducted within the program 'the Frontier Carbon Technologies' cosigned to the Japan Fine Ceramic Foundation from the New Energy and Industrial Technology Development Organization whose sponsorship is greatly acknowledged.

References

1 De Beers Industrial Diamond Division Ltd., *Ger. Pat.*, 2806070, 1979; R. J. Wedlake and A. L. Penny, *Chem. Abstr.*, 1979, **90**, 42865Z.
2 A. R. Badzian, *Mater. Res. Bull.*, 1981, **16**, 1385.
3 T. Komatsu, M. Nomura, Y. Kakudate and S. Fujiwara, *J. Mater. Chem.*, 1996, **6**, 1799.
4 R. Sen, B. C. Satishkumar, A. Govindaraj, K. R. Harikumar, G. Raina, J. P. Zhang, A. K. Cheetham and C. N. R. Rao, *Chem. Phys. Lett.*, 1998, **287**, 671.
5 J. Yu, J. Ahn, S. F. Yoon, Q. Zhang, Rusli, B. Gan, K. Chew, M. B. Yu, X. D. Bai and E. G. Wang, *Appl. Phys. Lett.*, 2000, **77**, 1949.
6 T. Y. Kosolapova, G. N. Makarenko, T. I. Serebryakova, E. V. Prilutskii, O. T. Khorpyakov and O. I. Chernysheva, *Poroshk. Metall. (Kiev)*, 1971, **1**, 27.
7 M. Kawaguchi and T. Kawashima, *J. Chem. Soc., Chem. Commun.*, 1993, 1133.
8 L. Maya and L. A. Harris, *J. Am. Ceram. Soc.*, 1990, **73**, 2498.
9 J. Bill, M. Friess and R. Riedel, *Eur. J. Solid State Inorg. Chem.*, 1992, **29**, 195.
10 Y. Goto, M. Sasaki, M. Hashizume and M. Suzuki, *J. Eur. Ceram. Soc.*, 1999, **19**, 2695.
11 A. R. Badzian, T. Niemyski, S. Appenheimer and E. Oluksnik, *Khim. Svyaz. Poluprovodn. Polumet.*, 1972, 362.
12 R. B. Karner, J. Kouvetakis, C. E. Warble, M. L. Sattler and N. Bartlett, *Mater. Res. Bull.*, 1987, **22**, 399.
13 J. Kouvatakis, T. Sasaki, C. Shen, R. Hagiwara, M. Lerner, K. N. Krishnan and N. Bartlett, *Synth. Met.*, 1989, **34**, 1.
14 A. Derre, L. Filipozzi, F. Bouyer and A. Marchand, *J. Mater. Sci.*, 1994, **29**, 1589.
15 M. Kawaguchi, T. Kawashima and T. Nakajima, *Chem. Mater.*, 1996, **8**, 1197.
16 R. Sen, B. C. Satishkumar, A. Govindaraj, K. R. Harikumar, M. K. Renganathan and C. N. R. Rao, *J. Mater. Chem.*, 1997, **7**, 2335.
17 M. Terrones, P. Redlich, N. Grobert, S. Trasobares, W. Hsu, H. Terrones, Y. Zhu, J. P. Hare, C. L. Reeves, A. K. Cheetham, M. Ruhle, H. W. Kroto and D. R. M. Walton, *Adv. Mater.*, 1999, **11**, 655.
18 T. Komatsu, *Macromol. Chem. Phys.*, 2001, **202**, 19.
19 T. Komatsu, *J. Mater. Chem.*, 2001, **11**, 802.
20 T. Komatsu and T. Nakamura, *J. Mater. Chem.*, 2001, **11**, 474.
21 M. Bonamico, V. Fares, A. Flamini and P. Imperatori, *J. Chem. Soc., Perkin Trans. 2*, 1990, **1**, 121.
22 A. Y. Liu, R. M. Wentzcovitch and M. L. Cohen, *Phys. Rev. B*, 1989, **39**, 1760.
23 Y. Miyamoto, A. Rubio, M. L. Cohen and S. G. Louie, *Phys. Rev. B*, 1994, **50**, 4976.
24 Y. Miyamoto, A. Rubio, M. L. Cohen and S. G. Louie, *Phys. Rev. B*, 1995, **52**, 14971.
25 P. Redlich, J. Loeffler, P. M. Ajayan, J. Bill, F. Aldinger and M. Ruhle, *Chem. Phys. Lett.*, 1996, **260**, 465.
26 K. Suenaga, C. Colliex, N. Demoncy, A. Loiseau, H. Pascard and F. Willaime, *Science*, 1997, **278**, 653.
27 P. K. Redlich, M. Terrones, C. M. Diego, W. K. Hsu, H. Terrones, M. Ruhle, H. W. Kroto and D. R. M. Walton, *Chem. Phys. Lett.*, 1999, **310**, 459.